

INFLUENCE OF CARBIDE DISTRIBUTION ON DUCTILITY OF HAYNES®282® FORGINGS

C Joseph¹, M. Hörnqvist², R. Brommesson³, C Persson¹

¹Chalmers University of Technology, Department of Materials and Manufacturing Technology, S-41296 Göteborg, Sweden

²Chalmers University of Technology, Department of Applied Physics, S-41296 Göteborg, Sweden

³Chalmers University of Technology, Department of Applied Mechanics, S-41296, Göteborg, Sweden

Keywords: Haynes®282®, forging, anisotropic ductility

Abstract

Haynes®282®, a relatively new superalloy is used in gas turbines in form of sheets, plates and forgings. Forgings undergo a series of deformation steps at high temperatures to form complex shapes of components. The deformation on forgings, changes the microstructural features and their distribution, and any change in distribution of microstructural features can affect the mechanical properties of the material. The present study is undertaken to investigate the possible causes of anisotropy in mechanical properties of a Haynes®282® forging through optical and electron microscopy. Microscopic investigations show that ductility is anisotropic and changes from 15% to 21%. The electron backscattered diffraction (EBSD) investigation reveals that the presence of carbide stringers (banding of MC and M₆C carbides) is associated with fine grains, thereby giving a bimodal distribution of grain size. Carbide stringers follow the complexity of forgings and are identified as the primary cause for the anisotropic behavior in ductility. Furthermore, micromechanical simulations of carbide stringers in association with a bimodal grain structure was seen to qualitatively correspond to the experimental observation indicating improved ductility with banding along the tensile axis

Introduction

Wrought nickel base alloys possess mechanical properties that enable them to withstand high stresses at elevated temperatures. These properties have made the alloys attractive for applications as components in aero and land-based gas turbines. One of the recently developed wrought alloys in this class of material is Haynes®282®. Haynes®282® has attracted interest because of its high temperature creep properties, good tensile strength, and easier fabricability than other comparable alloys such as Waspaloy and Rene 41 [1, 2]. This new alloy can be used in several forms such as sheets, plates and complex forgings depending on the application. Sheets, plates and forgings may show anisotropy in mechanical properties. Sheets and plates show fairly predictable behavior, especially in-plane, while forgings may exhibit strong inhomogeneous anisotropy in mechanical properties due to the complex shape and alteration of microstructure during forming. Several factors affecting mechanical properties of nickel base alloys have been presented and discussed in literature over the years. Some of the commonly identified factors are heat treatment time and temperature, precipitation of undesirable phases, processing temperature and time. These factors can alter the microstructure and thus affect the properties. Deridder et al. have shown that problems such as forging difficulties, elemental segregation and variation in mechanical properties increase, as the complexity of alloying elements increases. This variation in mechanical properties could be improved considerably through a combination of thermal treatment and controlled forging deformation [3]. Muzyka et al. found that microstructure and

properties of wrought superalloys can be controlled by precipitated phases [4]. Liu et al. found that morphology, size and distribution of precipitated MC carbide phase changes with change in solidification temperature [5]. It has also been shown that shape, size, and morphology of precipitated carbides also affects the room and high temperature properties of these nickel base alloys [6-7]. Baldan showed that the sensitivity of creep ductility is influenced by carbide dispersions due to cavity development at fracture [8]. Donachie et al. discusses the interrelationship between the forging and heat treatment practice to the impact resistance of forged Waspaloy at room temperature. They showed that impact resistance reduces due to presence of MC carbide films in the grain boundaries [9]. Recently, Joseph et al. observed anisotropic ductile behavior for room temperature tensile tested specimens in Haynes®282® forgings, varying from 24 % to 14 % as alignment of primary (MC) and secondary carbides (M₆C) stringers change from inclination of 45° to 90° with respect to tensile axis [10].

Although a large number of investigations have been performed on nickel base alloys, a little is known about the variation in mechanical properties of Haynes 282. The main objective of this article is to identify and understand the anisotropy in mechanical properties of a Haynes®282® forging. In this study, the microstructural investigations in closely spaced samples from a forging are presented and discussed. Additionally, micromechanical modeling is used in an attempt to describe the effects of the observed microstructural features on the tensile ductility.

Experimental procedure

In this study a Haynes®282® forging, with chemical composition according to Table I, was used. The final geometry, shown schematically in Figure 1, was processed from a billet with a nominal diameter of 152 mm, which was forged perpendicular to the billet axis down to a thickness of 90 mm at the thickest location. The forging was first, solution heat treated according to AMS 5915. It is subsequently heat treated at 1010 °C for 2 h followed by cooling at a rate equal to air cooling or faster and finally heat treated at 788 °C for 8 h and air cooled.

Table I. Composition (wt %) of the Haynes®282® alloy

Ni	Cr	Co	Mo	Ti
Bal	19.48	10.30	8.50	2.18
Al	Fe	C	B	Si
1.56	0.42	0.062	0.004	<0.05

Tensile specimens with a gauge diameter of 6.4 mm were machined from the heat treated forging at three locations, see Figure 1. Tensile testing was performed with universal testing machine at room temperature, at a strain rate of 0.005 /min to determine the yield strength (YS), and then at 0.5 /min until failure.

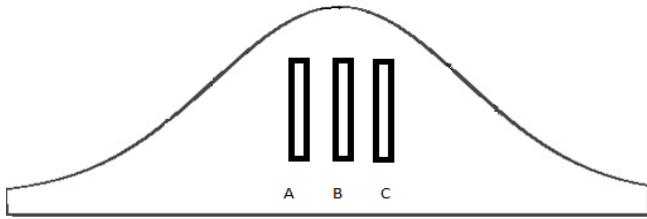


Figure 1. Schematic illustration of the forging geometry and the location of the extracted test specimens.

After tensile testing, fractography and metallography of the fractured specimens were performed to evaluate the microstructure. Longitudinal sections of the fractured samples were observed by optical and electron microscopy after grinding and polishing followed by electrochemical etching with oxalic acid at 3 V for 10–15 seconds (to reveal the grain boundaries). Additionally, EBSD measurement was also taken on longitudinal sections just below the fractured surface to analyze the grain orientation.

Results and Discussion

A fully heat-treated microstructure of Haynes 282, as shown in Figure 2(a), reveals presence of carbides such as MC carbides (rich in Ti and Mo) and M_6C carbides (rich in Mo) both at grain boundaries and within the grains. Additionally, $M_{23}C_6$ carbides (rich in Cr) are also present at the grain boundaries. The presence of yellow/orange colored carbo-nitride is also often seen. The primary strengthener in this alloy is the finely distributed gamma prime (γ') particles $Ni_3(Al/Ti)$ as shown in Figure 2(b). In all investigated specimens, the microstructure showed similar γ' precipitation and appearance of grain boundary carbides ($M_{23}C_6$). The average grain size measured in all specimens was around 200 μm .

Room temperature tensile testing was performed on specimens from the locations shown in Figure 1. Figure 3 shows mechanical test data for all specimens. The tensile test results show similar values of yield strength (YS) and ultimate tensile strength (UTS) for the three locations (A, B and C). However, the ductility drops considerably in specimen B (from 20 % to 15 %) while the values for A and C remains almost same (20 %). This shows that the measured ductility is anisotropic in contrary to the strength. The strength of the material is governed by γ' phase, which was homogeneous in the forging. However, the varying ductility can be due to several factors; like carbide stringers, grain orientation and grain size distribution.

Figure 4 shows an electron micrograph from a longitudinal section of the fractured specimen B from location B. The image confirms the presence of carbide stringers. The carbides (MC and M_6C) and carbo nitrides are seen to be distributed both inter- and intragranularly. The carbide stringers are aligned perpendicular to the tensile axis (black).

In the specimen from location A, the carbide stringers are inclined to the tensile axis (black), see Figure 5. During the conversion from ingot to billet, the local interdendritic segregation is aligned as a network of bands. The network of carbide bands further breakdown during subsequent forging operations, and the final distribution depends on the non-uniform plastic flow. The brittle carbides at grain boundaries crack prematurely under the applied load, constituting the weakest link in the microstructure. It is even possible that the carbides, being brittle at room temperature, might have internal cracks from the forging operations.

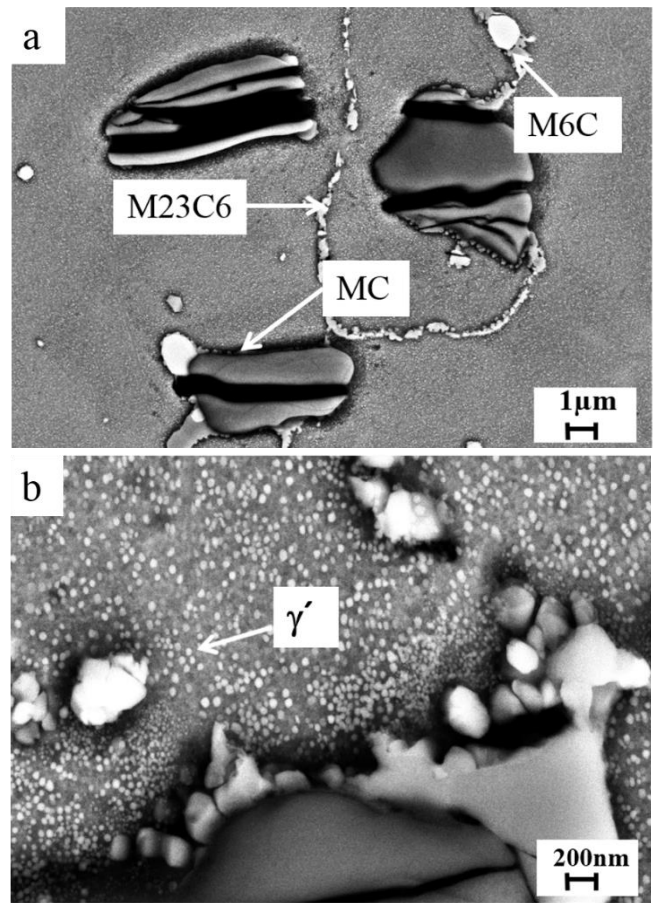


Figure 2. (a) Microstructure of Haynes[®]282[®] showing the presence of different carbides: MC carbides (rich in Ti and Mo), $M_{23}C_6$ (rich in Cr) and M_6C (rich in Mo) (b) Microstructure of Haynes[®]282[®] with distribution of fine spherical γ' ($Ni_3(Al/Ti)$)

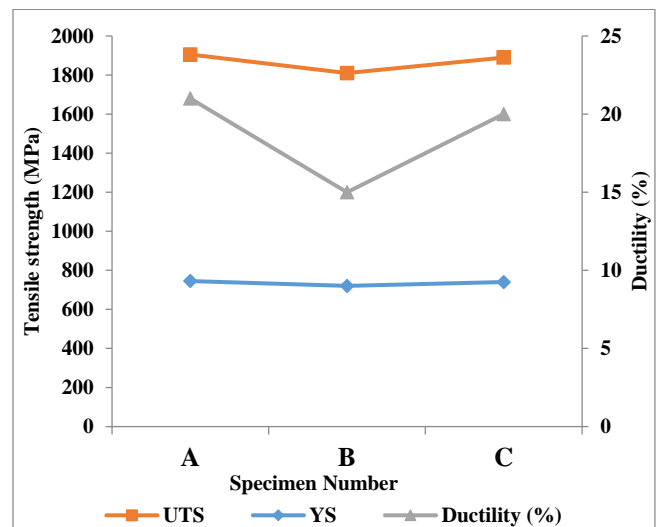


Figure 3. Room temperature tensile test results for specimens from the Haynes[®]282[®] forgings.

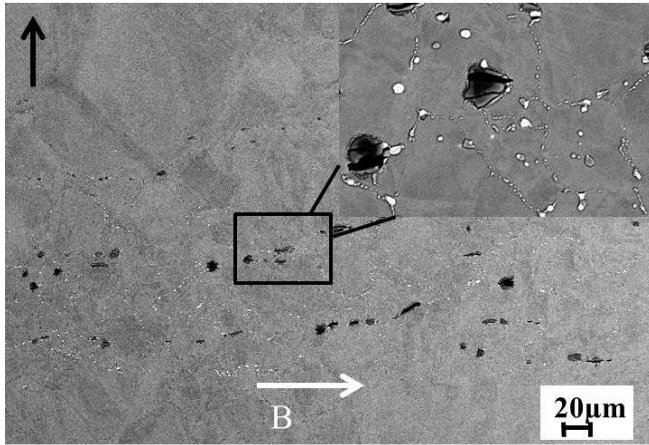


Figure 4. Longitudinal section of fractured specimen B showing the presence of carbide stringers aligned perpendicular to tensile axis (black). The insert shows a magnified view, where cracked carbides can be seen.

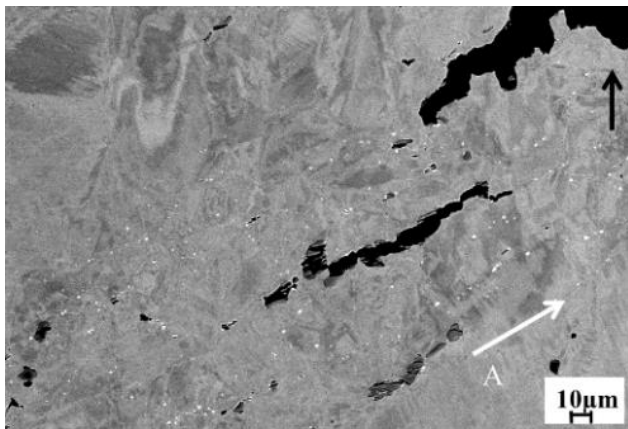


Figure 5. A longitudinal section of fractured specimen A showing the presence of carbide stringers inclined to tensile axis (black). The image shows crack initiation and propagation along carbide stringers.

The cracks further propagate easily through grain boundary by linking of fractured carbides, leading to an intergranular failure mode.

Figure 6 shows the optical micrographs of the microstructures of longitudinal sections below the fractured surfaces for specimens A and B. These microstructures reveal the presence of finer grains along the carbide stringers and coarser grains outside. Carbides at grain boundaries pin the boundaries and inhibit grain growth. Hence, the presence of carbide stringers leads to inhomogeneous grain growth during processing, and ultimately banding and a bimodal grain distribution. Finer grains in the order of a few microns can be detrimental when accompanied with carbide of a similar size. The carbide stringers of primary MC and M_6C follow the shape of the forging, and hence they are seen to be inclined (in case of specimen A) and perpendicular (in case of specimen B) with respect to tensile axis. The specimen C appears as a mirror image to specimen A.

Another potential effect of the bimodal grain size distribution could arise from the grain size dependence of the flow stress, since small

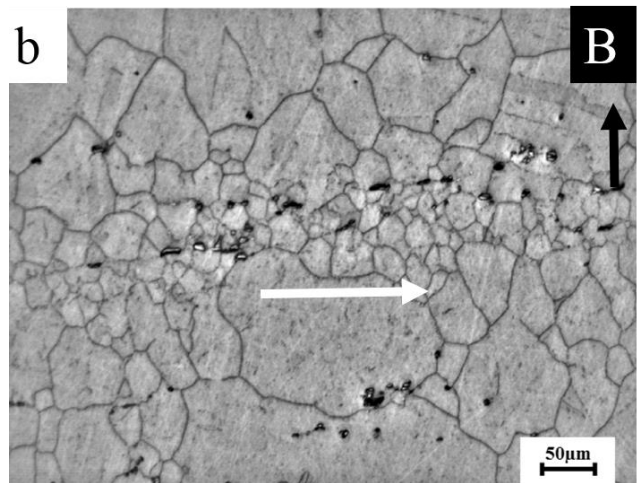
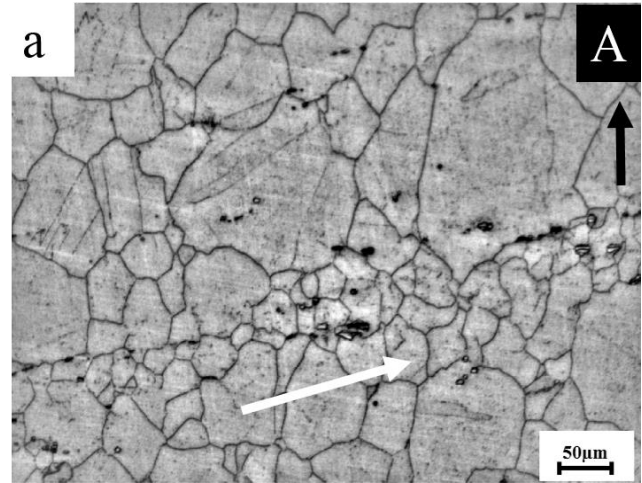


Figure 6. (a) Optical micrograph of specimen A showing presence of carbide stringers inclined to tensile axis. (b) Optical micrograph of specimen B showing presence of carbide stringers perpendicular to tensile axis. Both figures show a bimodal grain structure due to pinning of grain boundaries by carbides.

grains will have a larger resistance to plastic deformation. Figure 7 shows an inverse pole figure (IPF) map of a longitudinal section of specimen A (the tensile direction is vertical in the figure), where the banded bimodal grain size distribution can be clearly seen. If the grains are split into two subsets, depending on their size, it can be seen from the IPFs in Figure 7 that there is indeed a difference in the resulting deformation texture. Both subsets show dual $\langle 100 \rangle + \langle 111 \rangle // TD$ textures, as expected for axisymmetric tensile deformation of fcc materials. However, the overall texture strength and relative fiber strengths differ. The large grains show a much more pronounced texture, with a clear dominance by the $\langle 111 \rangle$ fiber. The small grains, on the other hand, show a less developed texture and almost equal fiber strengths. This is an indication of inhomogeneous deformation, where the large grained areas suffer more plastic straining during the test. The effect of the strain partitioning on the observed anisotropy is not clarified at present, but it can be expected to affect the stress concentration at the carbide particles in the bands. The fractographs for specimen A and B are shown in Figure 8. As can be seen in Figure 8(a) specimen A shows intergranular failure.

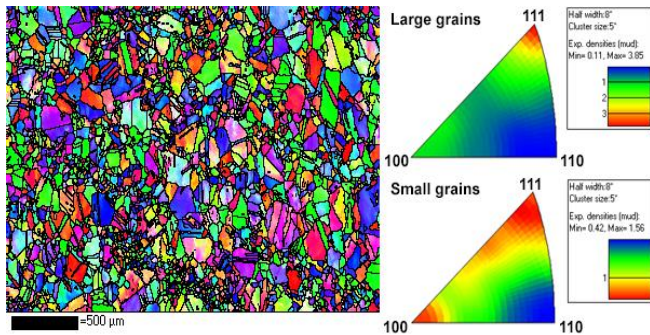


Figure 7. EBSD map of specimen A showing bimodal distribution of grain size and textures in the small and large grain areas. The inverse pole figures and the map show the direction of the tensile axis. The boundary between large and small grains were chosen to 50 μm , which gave a visually correct separation of the fine grained bands from the large grained areas.

Additionally, the presence of dimples and cracks in carbides is observed, indicating presence of ductile matrix with brittle carbides (Figure 8(b)). Also in specimen B, shown in Figure 8(c) and 8(d), the fracture is intergranular.

The dimpled features on fracture surface show the presence of relatively large MC carbides. The fracture surface of specimen C was similar to that of specimens A and B, with predominant dimpled features and cracked carbides. As can be seen, grain boundaries are the weakest link in the microstructure, and carbides are brittle phases when compared to the matrix. When the carbides at the grain boundaries fail, the crack propagates through the grain boundary and finally the material fails intergranularly.

An attempt to model the effect of carbide precipitates in association with the bimodal structure on tensile ductility was made by Brommesson and Joseph [11]. By modeling the microstructure using Voronoi tessellation [12] the bimodal grain size distribution was accounted for. Furthermore, the material behavior of the grains was modeled using a crystal plasticity model [13] and cohesive elements were embedded in the grain boundaries [14] to account for the observed intergranular fracture. The effect of carbides on the intergranular fracture was simulated by weakening the material behavior of the cohesive elements at grain boundaries where a higher concentration of carbides could be assumed from the experimental investigation, i.e. grain boundaries were selected based on orientation and size of adjacent grains. At such boundaries, the cohesive strength was reduced by 30 % for normal tension and by 10 % for shear deformation.

In this paper the modeling framework introduced in Brommesson and Joseph [11] is used and grain structure models with bands of smaller grains are investigated. The bands are given orientations of 45, 60 and 90° with respect to the tensile axis. In Figure 9 examples of the Voronoi grain structure models are shown. For each orientation five structures with statistically equivalent geometrical features are simulated and the mean stress responses from these simulations are given in Figure 10(a). Figure 10(a) clearly shows that a more brittle response is obtained for an orientation of 90° of the band with smaller grains compared to orientations of 45 and 60°.

The ductility, measured as the engineering strain at which the stress has decreased to 70 % of the UTS for each simulation, is given in Figure 10. It can be observed that there is a scatter in the simulation results. This scatter is caused by the statistical nature of the grain structure model generation. The ductility obtained from the

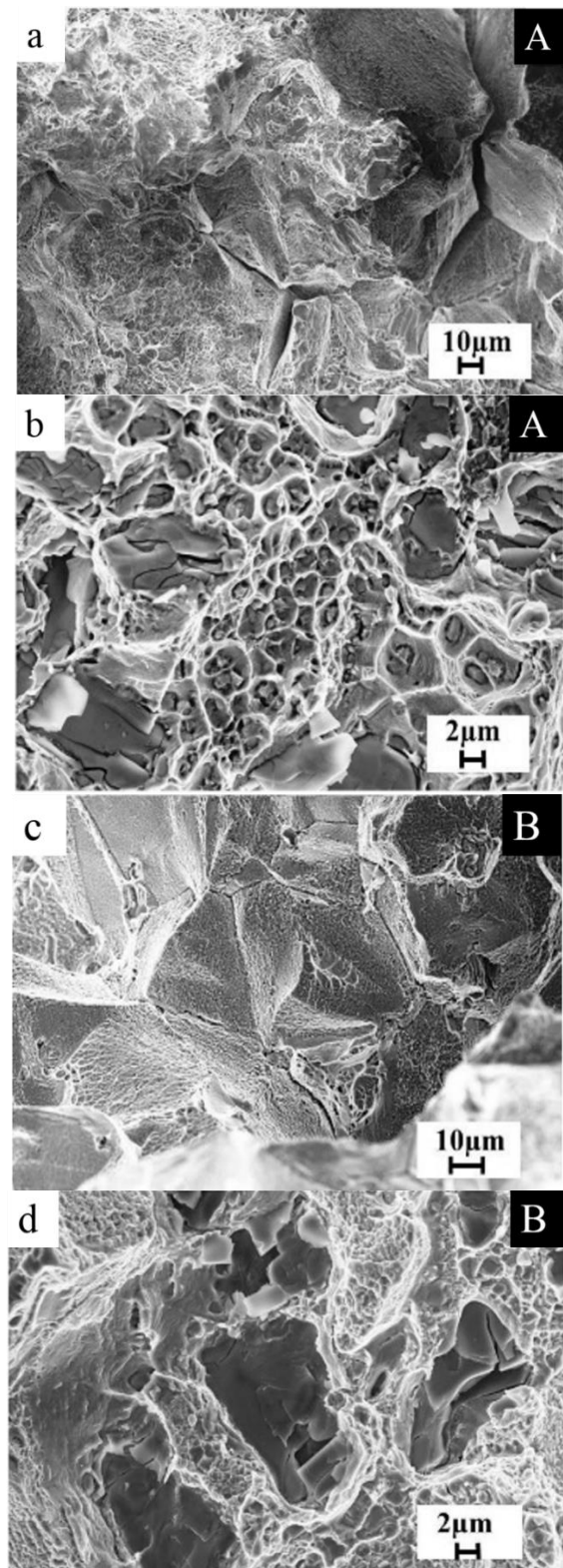


Figure 8. (a) Fractograph of specimen A showing intergranular failure (b) Presence of dimples on the fracture surface of specimen A and brittle failure of MC carbides. (c) Fractograph of specimen B showing intergranular failure (d) Fractograph showing presence of dimples on the fracture surface of specimen B and cracked larger MC carbides.

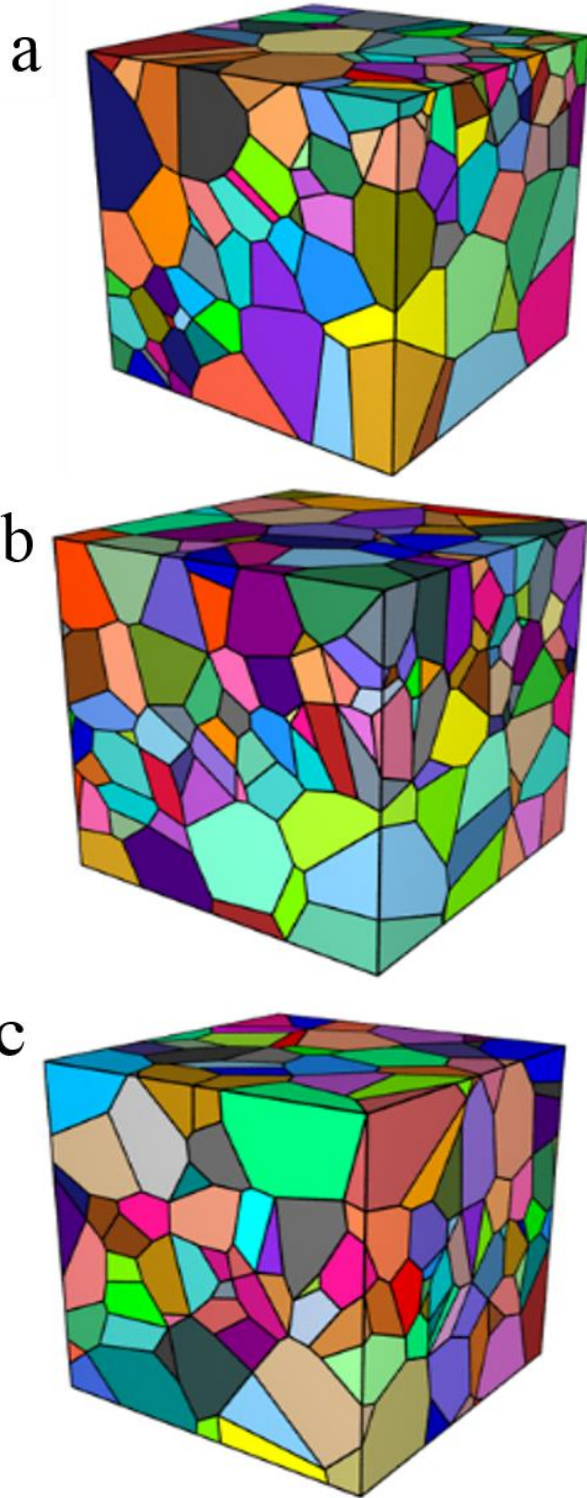


Figure 9. Grain structure models with (a) a band of smaller grains oriented 45° , (b) a band of smaller grains oriented 60° and (c) a band of smaller grains oriented 90° with respect to the (vertical) tensile axis.

simulations are closely related to the preferred crack path in each grain structure, which in turn depends on the size, geometry,

orientation of the grains, and the stress distribution within the grain structure.

In Figure 11 an example of the crack path in a grain structure with a band orientation of 90° is shown, where the straight crack plane gives a brittle behavior [11]. Although there is a scatter in the simulation results, the trend of an improved ductility is evident for simulations with a steeper angle of the band with respect to the tensile axis.

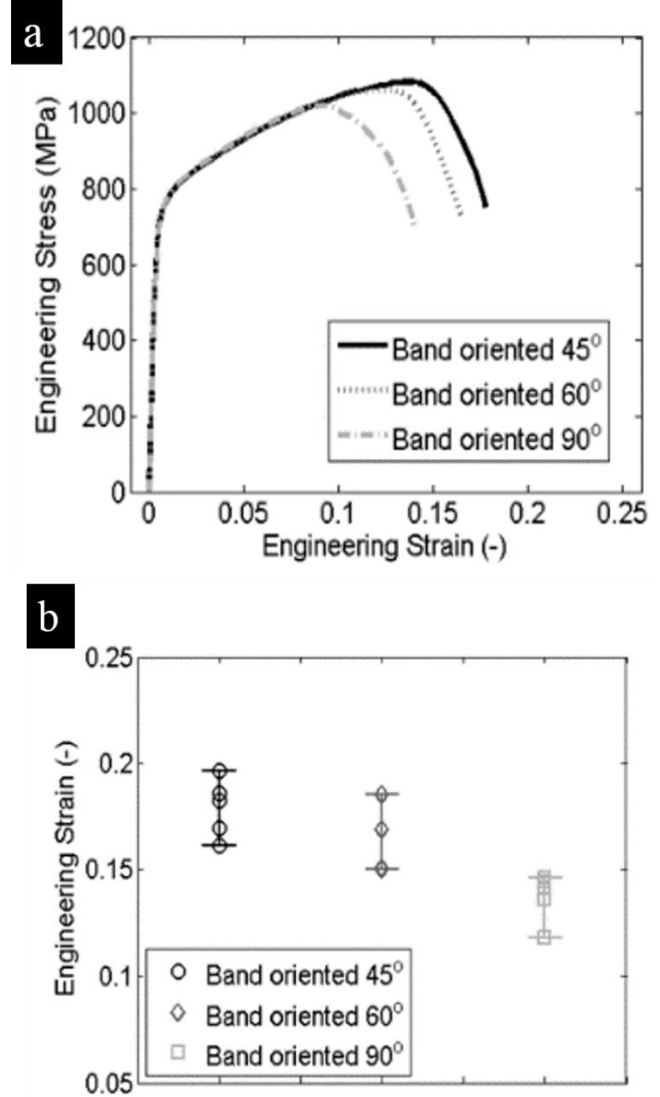


Figure 10. Simulation results for grain structures with three different orientations of the bands with smaller grains. (a) The mean values of the stress response for five simulations for each band orientation. (b) The ductility from each simulation measured as the engineering strain at 70 % of UTS.

Conclusion

In summary, this study shows that the forging practice and heat treatment adopted here gives uniform yield strength of Haynes 282, arising from the homogeneous distribution of the γ' phase. The ductility, on the other hand, showed marked anisotropy. This was

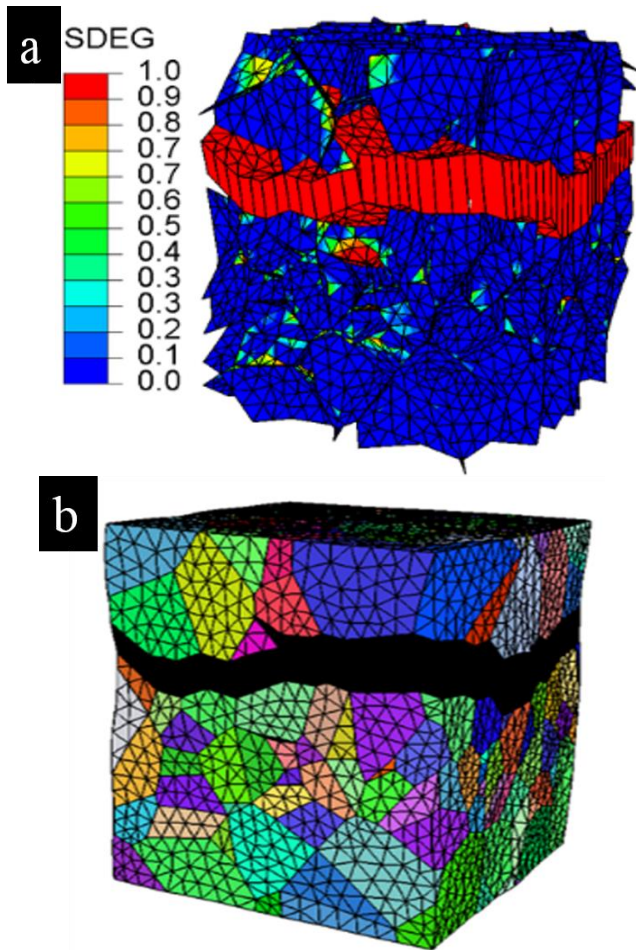


Figure 11. An example of a crack in a grain structure model with a band of smaller grains oriented 90° with respect to the tensile axis. (a) The resulting damage field for the cohesive elements (with a scalar damage variable, SDEG, on a scale [0,1] ranging from undamaged to completely damaged elements). (b) The deformed grain structure model showing colored grains, element mesh and black surface.

attributed to the presence of carbide stringers formed during forging due to local elemental segregation in the ingot. These carbide stringers pin the grain boundaries and give a banded bimodal grain size distribution. Fracture initiates on cracking of the carbides in the stringers, and propagate by linking of fractured carbides through tearing of grain boundaries. The preferential alignment of carbide stringers relative to the tensile axis controls the tensile ductility. It was also seen that the deformation preferentially occurred in the large grained areas as compared to the band of small grains associated with the carbide stringers. However, the relative contribution of the inhomogeneous deformation to the observed anisotropy is not clear at present. The observed anisotropy was qualitatively captured by a micromechanical grain scale model based on crystal plasticity and cohesive zones, where the presence of banded structure and weakening of grain boundaries due to carbides were explicitly treated.

Acknowledgment

This work has been funded by the Swedish National Aeronautical Research Program (NFFP6) which is gratefully acknowledged. We

would also like to thank Bengt Pettersson and Frank Skystedt at GKN Aerospace for their valuable comments on the manuscript.

References

1. L.Pike, "Haynes[®]282[®] alloy, a new wrought superalloy designed for improved creep strength and fabricability," *Proceedings of the ASME turbo Expo 4*, (2006), 1031-1039.
2. L.Pike, "Development of a fabricable gamma prime strengthened superalloy," *Proceedings of the International Symposium on superalloys*, (2008), 191-200.
3. A.J.DeRidder and R.W.Koch, "Controlling variations in mechanical properties of heat resistant alloys during forging," *Metals Engineering quarterly American society for metals*, (1965), 61-64.
4. D.R.Muzyka, "Controlling microstructures and properties of superalloys via use of precipitated phases," *Metals engineering quarterly*, (1971), 12-19.
5. L.Liu and F.Sommer, "Effect of solidification conditions on MC carbides in a nickel base superalloy IN738LC," *Scripta Metallurgica*, 30, (1994), 587-591.
6. Jinxia Yang et al., "Relative stability of carbides and their effects on the properties of K465 superalloy," *Material science and engineering A*, 429, (2006), 341-347.
7. J.S.Bae et al., "Formation of MC- γ/γ' eutectic fibers and their effect on stress rupture behavior in D/S Mar-M247LC superalloy," *Scripta Materialia*, 45, (2001), 503-508.
8. A.Baldan, "Effect of carbides and cavitation on the Monkman-grant ductility of a nickel base superalloy," *Journal of Materials Science letters*, 11,(1992),1315-1318.
9. M.J.Donachi et al., "Effect of hot work on the properties of Waspaloy," *Metallurgical Transactions*, 1, (1970) 2623-30.
10. C. Joseph et al., "Anisotropy of room temperature ductility of Haynes[®]282[®] forgings," *8th International symposium on superalloy 718 and Derivaties*, John Wiley and Sons, Inc. Hoboken, NJ, USA, (2014).

11. R.Brommesson et al., "3D grain structure modelling of intergranular fracture in forged Haynes 282," *Engineering Fracture Mechanics*, 154, (2016), 57-71.
12. R.Quey, P. Dawson, F. Barbe, "Large-scale 3D random polycrystals for the finite element method: Generation, meshing and remeshing," *Comput. Methods Appl. Mech. Engrg.* 200, (2011), 1729-1745.
13. M.Ekh, R. Lillbacka, K. Runesson, "A model framework for anisotropic damage coupled to crystal (visco) plasticity," *Int. J. Plasticity*, 20, (2004), 2143-2159.
14. K.Carlsson, "Modeling of three dimensional microstructures including grain boundary mechanisms," *Master's thesis, Applied Mechanics, Chalmers University of Technology* (2013), 51.